Electronic Supplementary Information

Interconvertible Multiple Photoluminescence Color of a Gold(I) Isocyanide Complex in the Solid State: Solvent-Induced Blue-Shifted and Mechano-Responsive Red-Shifted Photoluminescence

Tomohiro Seki,[1] Taichi Ozaki,[1] Takuma Okura,[1] Kiyotaka Asakura,[2] Aya Sakon,[3] Hidehiro Uekusa,[3]* and Hajime Ito[1]*

[1]Division of Chemical Process Engineering and Frontier Chemistry Center, Faculty of Engineering, Hokkaido Uiversity, Sapporo, Hokkaido 060-8628, Japan
[2]Catalysis Research Center, Hokkaido University, Sapporo, Hokkaido, 001-0021, Japan
[3]Department of Chemistry and Materials Science, Graduate School of Tokyo Institute of Technology

Email: hajito@eng.hokudai.ac.jp

Contents

1. General

All commercially available reagents and solvents are of reagent grade and were used without further purification unless otherwise noted. Solvents for the synthesis were purchased from commercial suppliers, degassed by three freeze-pump-thaw cycles and further dried over molecular sieves (4 Å). NMR spectra were recorded on a JEOL JNM-ECX400P or JNM-ECS400 spectrometer (^{1}H: 400 MHz) using tetramethylsilane and $CDCl_3$ as internal standards, respectively. Emission spectra were recorded on a Hitachi F-7000 spectrometer. Fluorescence microscopic spectra were recorded on a Photonic Hamamatsu PMA-12 Multichannel Analyzer. The emission quantum yields of the solid samples were recorded on a Hamamatsu Quantaurus-QY spectrometer with an integrating sphere. Emission lifetime measurements were recorded on a Hamamatsu Quantaurus-Tau spectrometer. Elemental analyses and low- and high resolution mass spectra were recorded at the Center for Instrumental Analysis, Hokkaido University. Photographs were obtained using Olympus BX51 or SZX7 microscopes with Olympus DP72, Nikon D5100 or RICOH CX1 digital cameras. Powder diffraction data were recorded at room temperature on a Rigaku SmartLab diffractometer with Cu Kα radiation and a D/teX Ultra detector covering 5–60° (2θ). Simulated powder patterns of **2B**, **2G**, and **2Y** (Figures S6 and S7) were generated with Mercury 3.0 from the structures determined by single crystal and powder X-ray diffraction analyses.[S1]

2. Interconversion of 2B, 2G, 2Y, and 2O

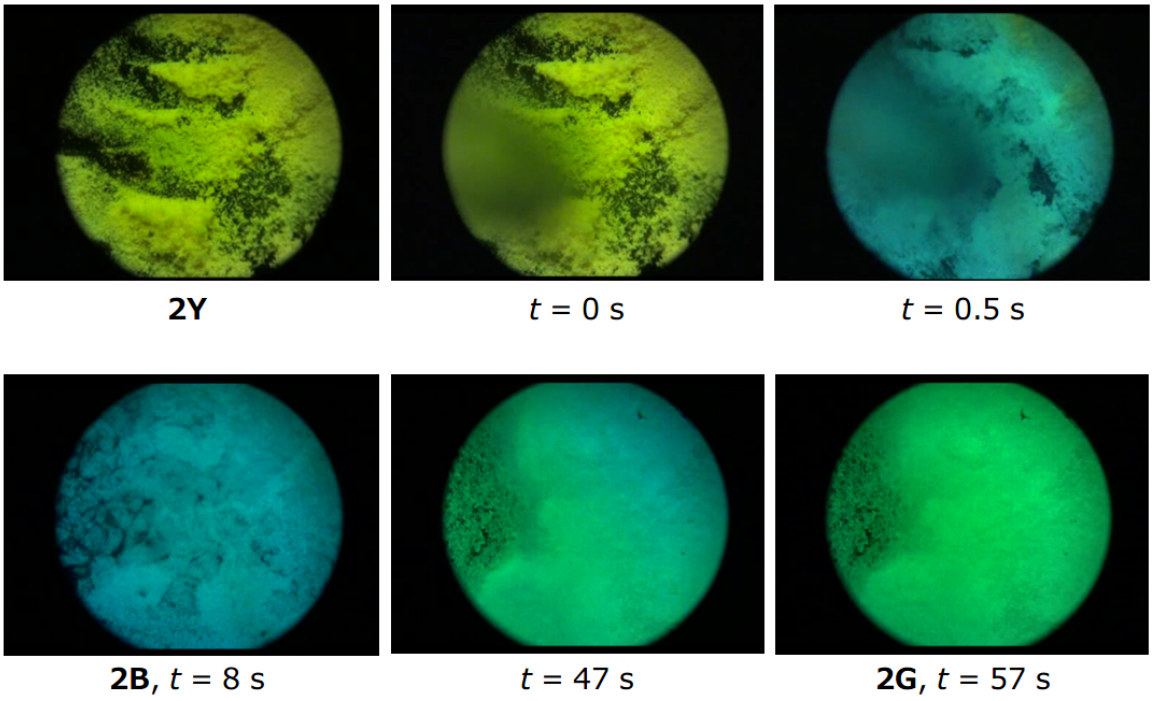

Fig. S1 A series of photographs of acetone-induced emission color change of **2Y** taken under UV light. Acetone was added at t = 0 s and emission color immediately changed to blue due to the formation of **2B**. After 47 s, emission color gradually changed to green due to the formation of **2G** upon drying acetone.

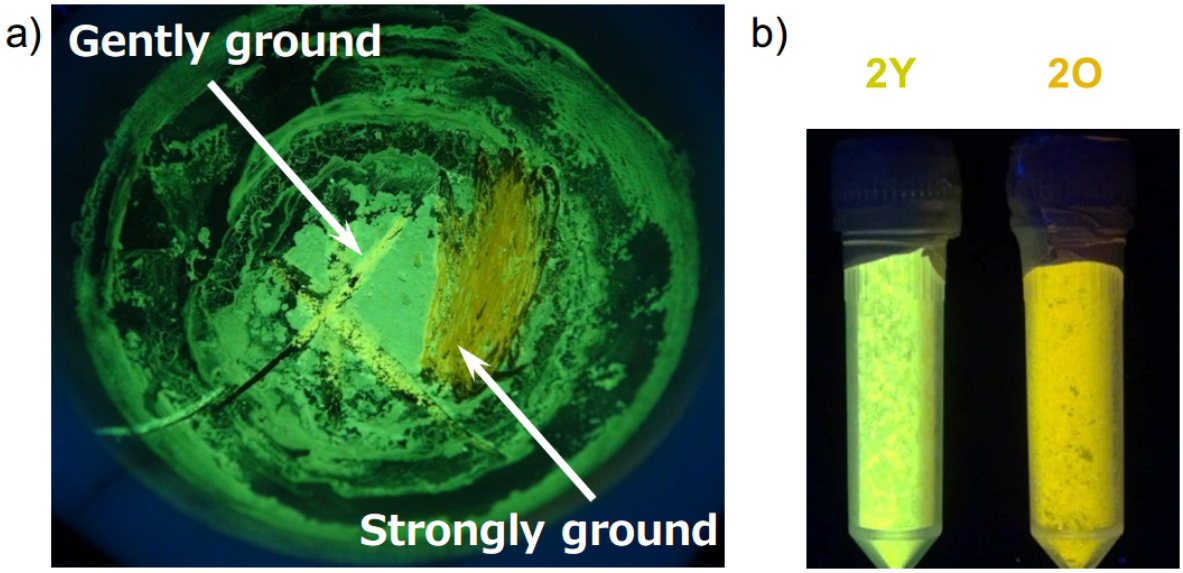

Fig. S2 a) Photograph of emission color changes of **2G** upon grinding with pestle taken under UV light. These emission color changes are caused by phase transitions: gentle grinding induces phase transition into **2Y**, while hard grinding induces phase transition into **2O**. b) Photograph of **2Y** and **2O** obtained by ball-milling of **2G** for 10 and 15 min, respectively, at a speed of 4600 rpm.

3. Photophysical Properties

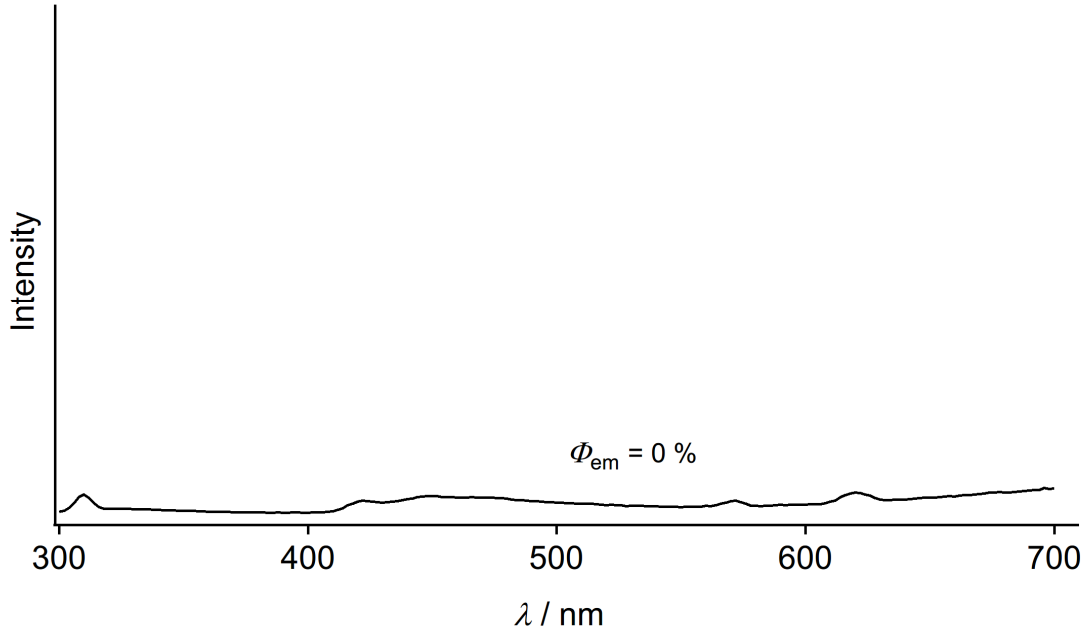

Fig. S3 Emission spectrum (λ_{ex} = 280 nm) of **2** in THF (c = 1.6 × 10^{-6} M) at room temperature.

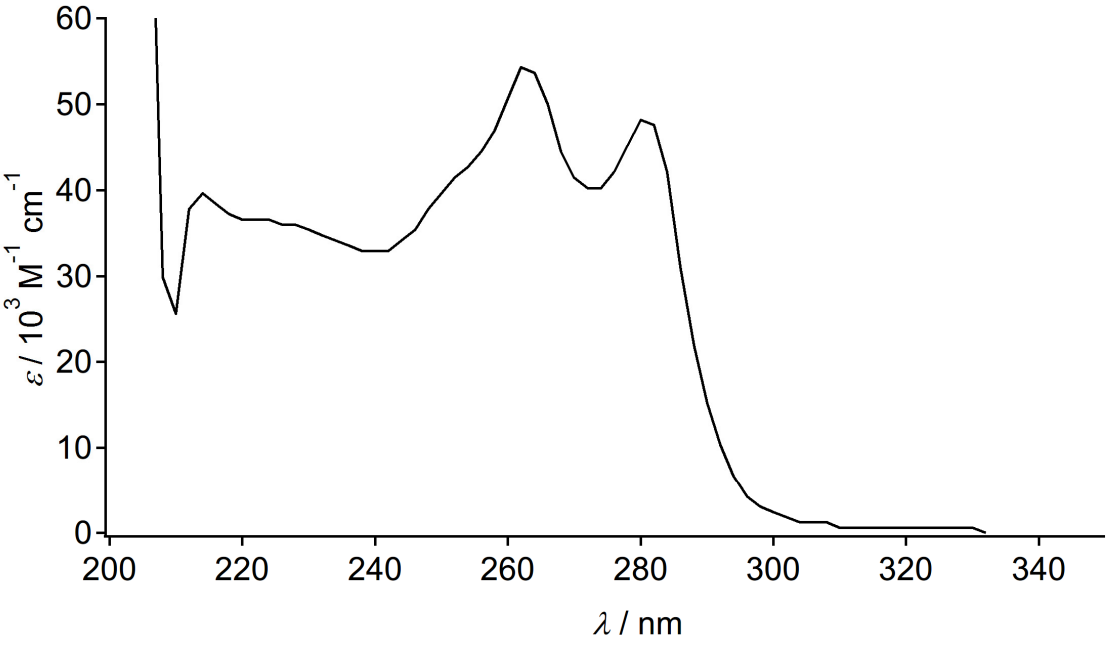

Fig. S4 UV/vis absorption spectrum of **2** in THF (c = 1.6 × 10^{-6} M) at room temperature.

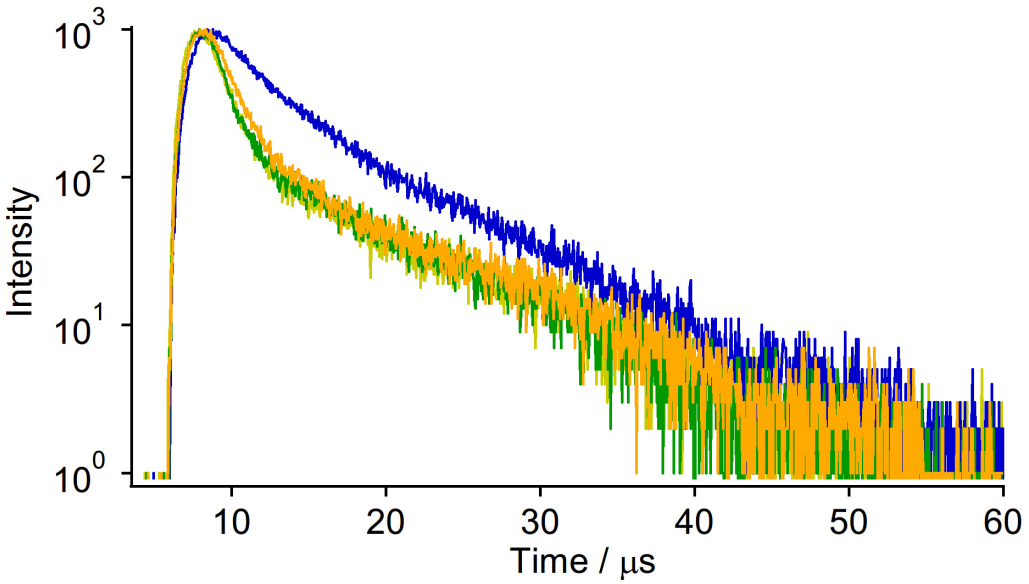

Fig. S5 a) Photoluminescence decay profiles of **2B** (blue line, λ_{em} = 490 nm), **2G** (green line, λ_{em} = 538 nm), **2Y** (yellow line, λ_{em} = 565 nm), and **2O** (orange line, λ_{em} = 620 nm) with an excitation at 370 nm.

Table S1 Photophysical properties of **2**

	Φ_{em} / % (λ_{ex} / nm)	τ_{av} / μs[a,b] (λ_{em} / nm)	τ_1 / μs (A / -)	τ_2 / μs (A / -)	k_r / 10^5 s^{-1}	k_{nr} / 10^5 s^{-1}
2B	10 (380)	2.55 (490)	0.879 (0.35)	3.45 (0.65)	4.3	12.2
2G	10 (415)	0.585 (538)	0.326 (0.97)	8.95 (0.03)	1.7	15.3
2Y	27 (397)	0.454 (565)	0.340 (0.62)	0.984 (0.38)	0.4	3.6
2O	30 (450)	0.611 (620)	0.212 (0.27)	0.758 (0.73)	6.6	15.4

[a]: λ_{ex} = 370 nm. [b]: $\tau_{av} = (\Sigma A_i\tau_i)/(\Sigma A_i)$.

4. PXRD Pattern of As-synthesized 2 and 2Y Obtained by Ball-Milling

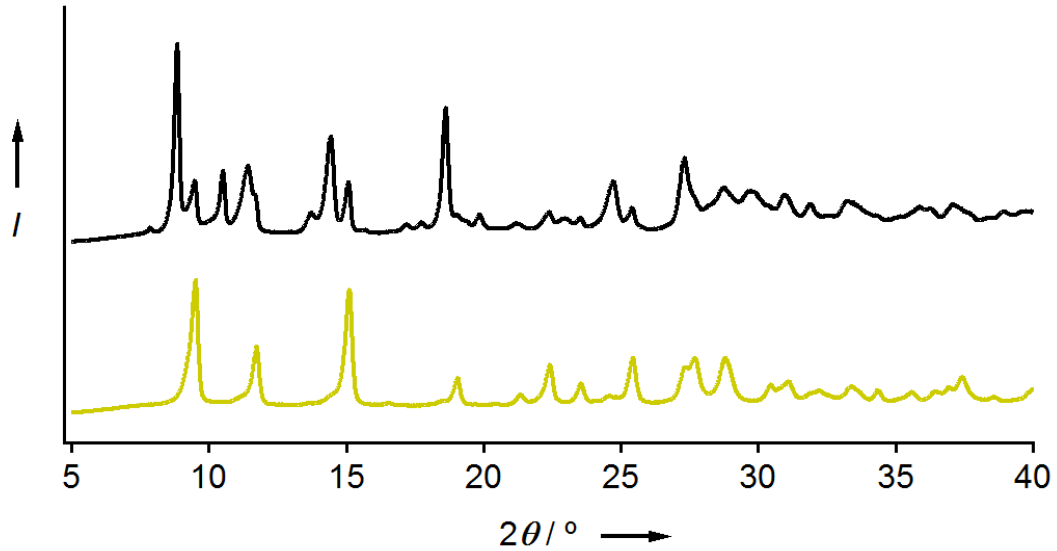

Fig. S6 PXRD patterns of as-synthesized powder of **2** (black line) and **2Y** obtained by ball milling (yellow line).

5. Data for Single Crystal and Powder X-ray Structural Analyses

Single crystal X-ray structural analyses: Single crystal X-ray diffraction data of the **2B** was recorded on a Rigaku R-AXIS RAPID (Mo Kα) and those of the **2G** was recorded on a Rigaku R-AXIS RAPID-II (Cu Kα). Each structure was solved by the direct methods with the program SHELXS-97[S2] and was refined by the full-matrix least-squares method with SHELXL-97.[S2] All the non-hydrogen atoms were refined with anisotropic temperature factors. The H atoms were located geometrically and were included in the least-squares calculations using the riding-atom model. Isotropic temperature factors constrained to $1.2U_{eq}$(C) were given to all hydrogen atoms. As for the **2G**, the solvent molecules (acetone and/or water molecules) were severely disordered in the 1-D channel along *a* axis (shown in Fig. S9) and couldn't be modeled. Therefore, the residual density of the disordered solvent molecules was treated by using the SQUEEZE procedure of PLATON[S3] and the final refinement was performed by using the squeezed *hkl* data. From the result of the SQUEEZE procedure, there are 17 electrons in the void of the unit cell (48.4 $Å^3$; 10.1%).

Preparation of single crystal of 2B for X-ray diffraction analyses: Single crystal **2B** was prepared from saturated acetone solution of **2**. The specimen crystal was coated with paratone oil just after took from acetone solution and its X-ray diffraction data were collected at 173(2) K under a stream of cold nitrogen gas.

Preparation of single crystal of 2G for X-ray diffraction analyses: Single crystal **2G** was prepared from single crystal **2B** under air or water vapor. After the crystal was exposed to air or water vapor for 1 week, single crystal X-ray diffraction measurement of **2G** was performed at 173(2) K under a stream of cold nitrogen gas.

Table S2 Summary of X-ray crystallographic data for **2B** and **2G**.

Polymorph	**2B**	**2G**
CCDC Name	CCDC 1035806	CCDC 1035808
Empirical Formula	$C_{24}H_{16}Au_2F_8N_4O_2$	$C_{18}H_4Au_2F_8N_4$
Formula Weight	938.34	822.18
Crystal System	triclinic	triclinic
Crystal Size / mm	0.060 × 0.030 × 0.010	0.032 × 0.029 × 0.010
a / Å	3.5452(4)	3.5707(3)
b / Å	14.0087(15)	10.3087(10)
c / Å	14.2490(15)	14.2742(11)
α / °	109.292(3)	107.689(4)
β / °	91.673(3)	92.505(5)
γ / °	91.322(2)	100.205(5)
V / Å^3	667.23(13)	489.99(8)
Space Group	P-1 (#2)	P-1 (#2)
Z value	1	1
D_{calc} / g·cm^{-3}	2.335	2.786
Temperature / K	173(2)	173(2)
$2\theta_{max}$ / °	27.464	68.208
μ / cm^{-1}	110.67 (MoKα)	285.92 (CuKα)
No. of Reflections Measured	Total : 6546 Unique : 3042 (R_{int} = 0.0514)	Total : 5156 Unique : 1750 (R_{int} = 0.1077)
Residuals: R_1 (I > 2.00σ (I)) / %	4.73	10.08
Residuals: wR_2 (All reflections) / %	10.55	25.46
Goodness of Fit (GOF)	1.152	1.114
Maximum peak in Final Diff. Map / Å^3	2.596 e$^-$	2.763 e$^-$
Minimum peak in Final Diff. Map / Å^3	–2.354 e$^-$	–3.642 e$^-$

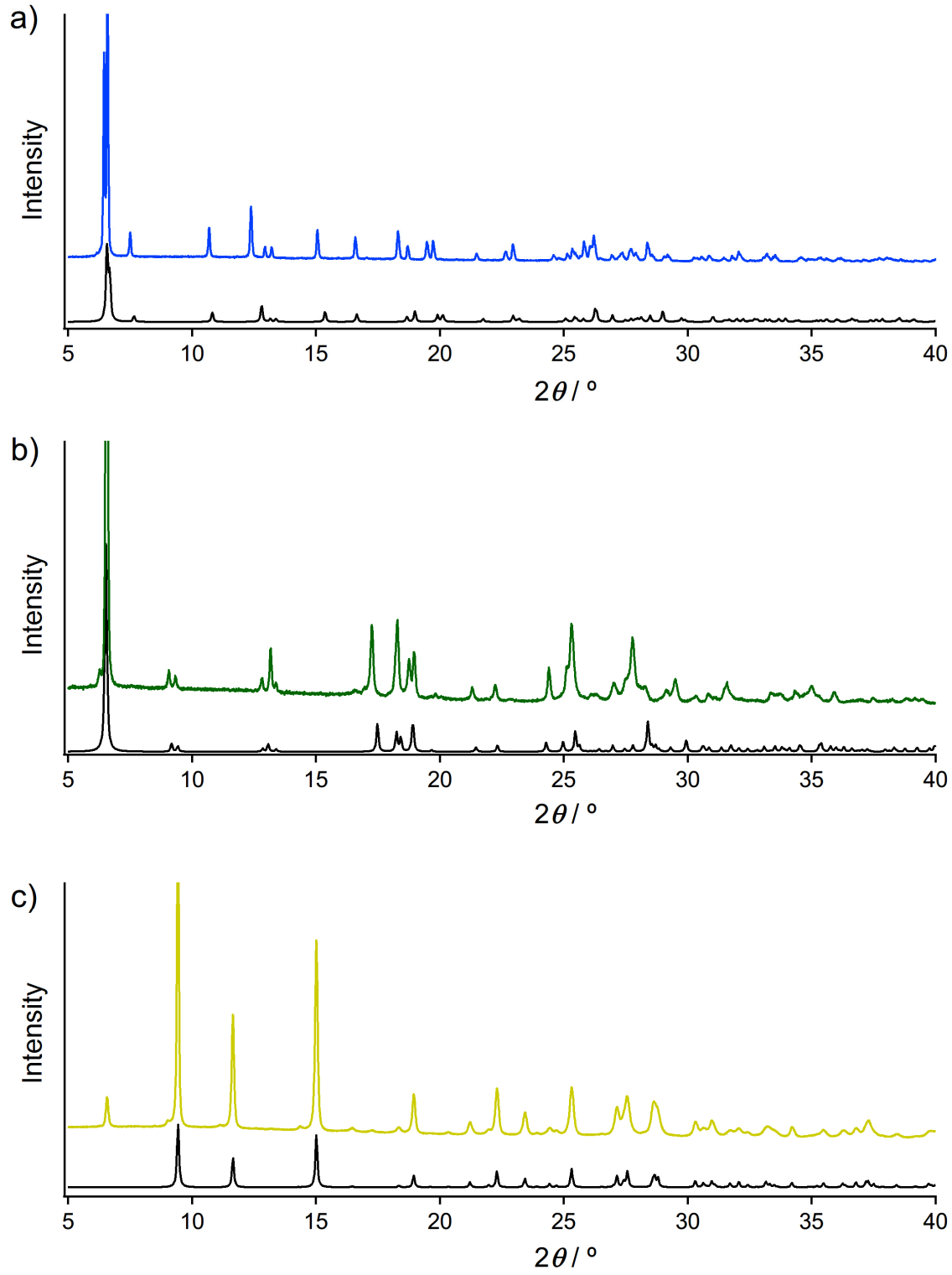

Fig. S7 a and b) Comparison of PXRD patterns (upper) and simulated powder patterns derived from the single crystal structures (lower) of **2B** (a) and **2G** (b). c) Comparison of PXRD pattern (upper) of **2Y** and simulated powder patterns derived from the *ab initio* PXRD analysis of **2Y**. A diffraction peak at 6.6° c) is derived from residual **2G** phase contaminated within **2Y** phase.

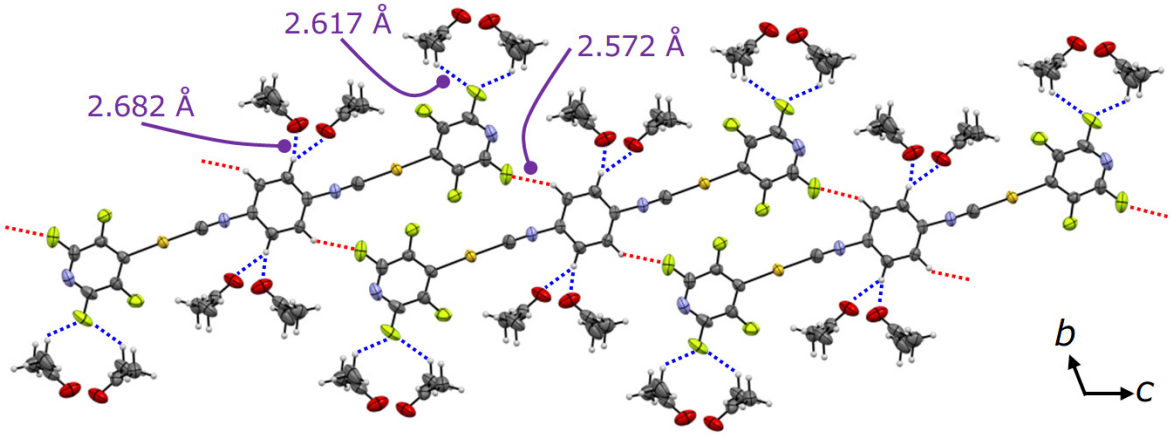

Fig. S8 ORTEP representation of packing structure of **2B** viewed along the direction of *a* axis. Intermolecular interactions between **2** molecules and between **2** molecule and acetone are shown by red and blue dotted lines, respectively.

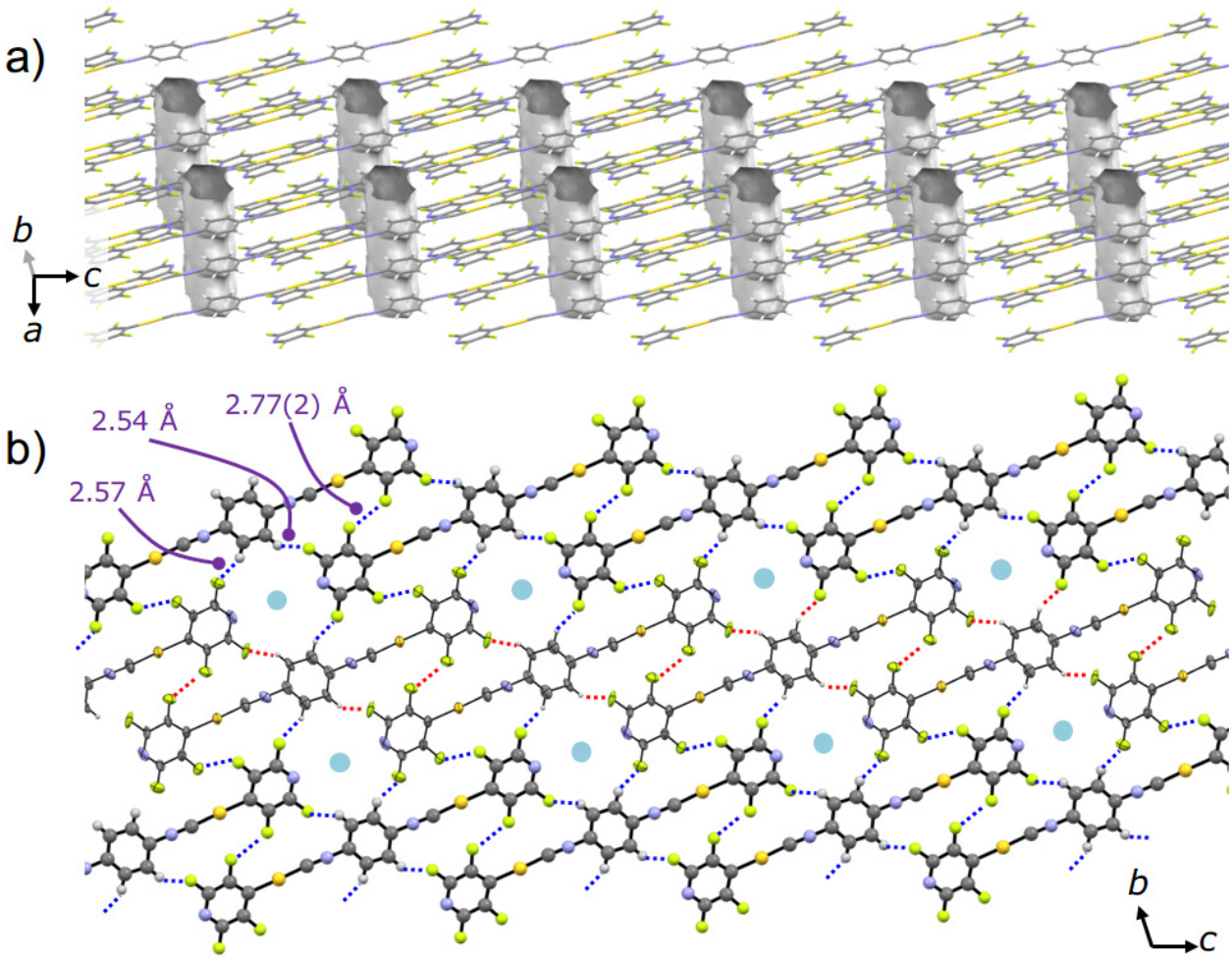

Fig. S9 a) Capped-stick representation of packing structure of **2G**. Empty void regions are depicted by gray polygons and have a volume of 48.4 Å^3 per unit cell, which occupies 10.1 % of the unit cell. In this region, acetone and/or water are accommodated to form 1-D channel running along the direction of *a* axis. b) Packing structure of **2G** viewed along the direction of *a* axis. Single molecular tape is shown by ORTEP representation and the two neighboring tapes are shown by ball-and-stick representation. Intermolecular interactions within a tape and between tapes are shown by red and blue dotted lines, respectively. Light blue circles represent empty void regions.

***Ab* initio crystal structure analysis of 2Y from powder X-ray diffraction data:** The powder X-ray diffraction pattern of **2Y** (yellow line in Fig. 4) was indexed using the program DICVOL04[S4] (M_{20} = 28.4[S5] F_{20} = 56.3[S6]), giving the following unit cell with monoclinic metric symmetry: a = 7.78 Å, b = 18.70 Å, c = 6.74 Å, β = 103.24° (V = 954.77 Å^3). From the systematic absences, the space group was assigned as $P2_1/c$. From the consideration of the unit cell volume (corresponding to Z = 2) and the molecular symmetry, Z'= 0.5 and the molecule is on the inversion center. The profile was fitted using the Pawley method[S7] in the program DASH[S8] gave a good quality of fit (R_{wp} = 7.13%). The simulated annealing structure solution calculation was carried out using the program DASH with 7 variables (comprised of three translational variables, three orientational variables and one torsion angle variable) being determined. The molecular model was taken from the crystal structure of **2B**. Subsequent Rietveld refinement[S9] was carried out using the GSAS[S10] program. In the Rietveld refinement, standard restraints were applied to bond lengths and bond angles, planar restraints were applied to the aromatic rings, and a global isotropic displacement parameter was also refined. The final Rietveld refinement (Fig. S10) gave the following parameters: a = 7.79058(18) Å, b = 18.7202(5) Å, c = 6.74157(17) Å, β = 103.167(3) °, V = 957.35(5) Å^3; R_{wp} = 4.62%, R_p = 3.60%, R_{F2} = 2.74% (2θ range: 7.00–60.00°; 5300 profile points; 107 refined variables; the corresponding R_{wp} for the Le Bail fitting was 3.60%).

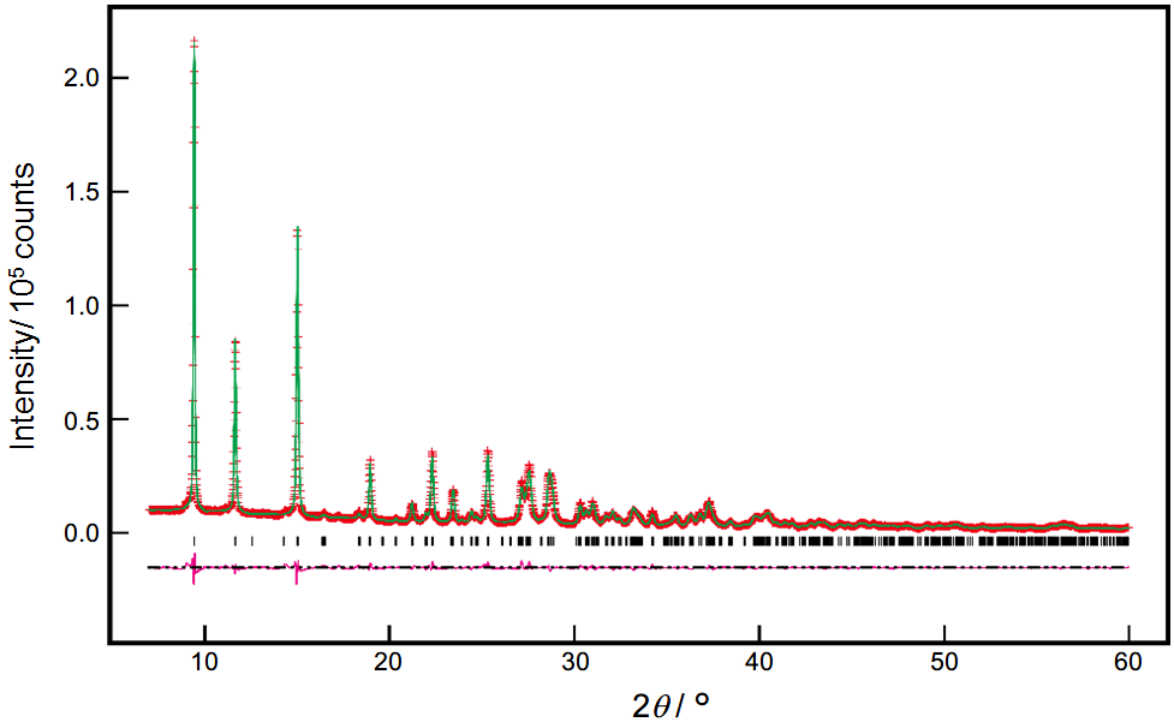

Fig. S10 Final Rietveld refinements for **2Y**, showing the experimental PXRD profile (red + marks), calculated PXRD profile (green solid line) and difference profile (lower pink line).

Table S3 Summary of X-ray crystallographic data for **2Y**.

Polymorph	**2Y**
CCDC Name	CCDC 1035810
Empirical Formula	$C_{18}H_4Au_2F_8N_4$
Formula Weight	822.18
Crystal System	monoclinic
a / Å	7.79058(18)
b / Å	18.7202(5)
c / Å	6.74157(17)
α / °	90
β / °	103.167(3)
γ / °	90
V / Å^3	957.35(5)
Temperature / K	293
Space Group	$P2_1/c$ (#14)
Z value	2
R_{wp} / %	4.62
R_p / %	3.60
R_{F2} / %	2.74

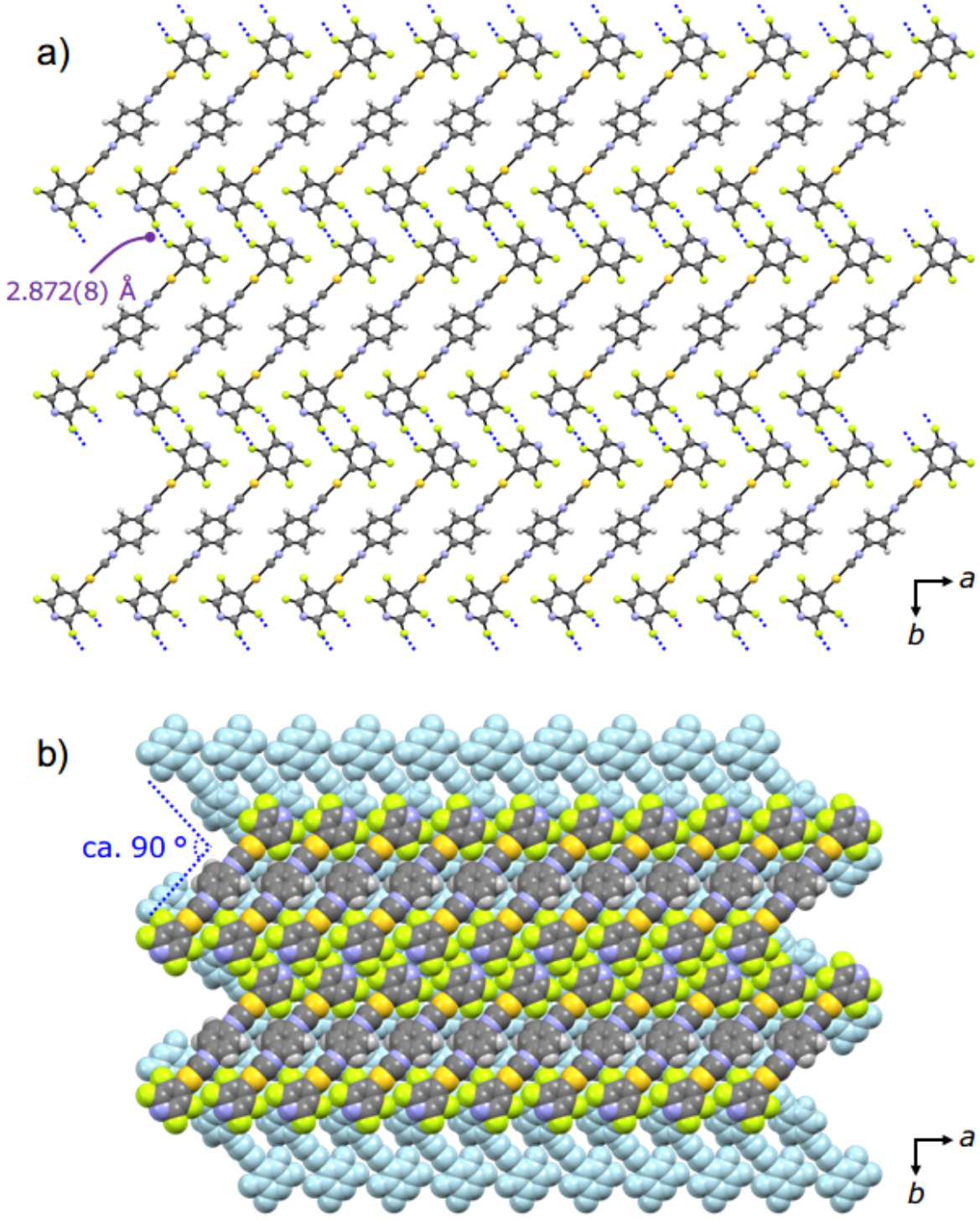

Fig. S11 a) Ball-and-stick representation of packing structure of **2Y** viewed along the direction of *c* axis. Intermolecular interactions between tapes are shown by blue dotted lines. b) Space-filling representation of packing structure of **2Y** viewed along the direction of *c* axis. Molecules in the second sheet were depicted by light blue.

6. Characterization of 2B, 2G, 2Y, and 2O

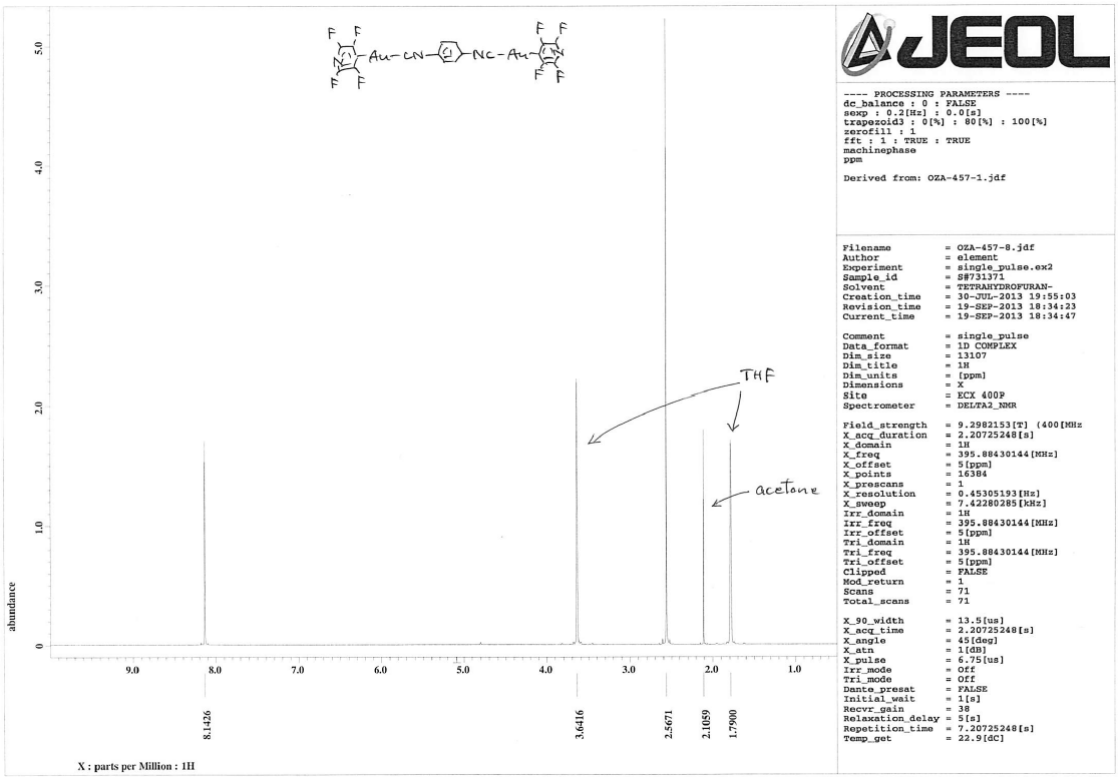

Fig. S12 ^{1}H NMR spectrum of **2G** dissolved in THF-d_8.

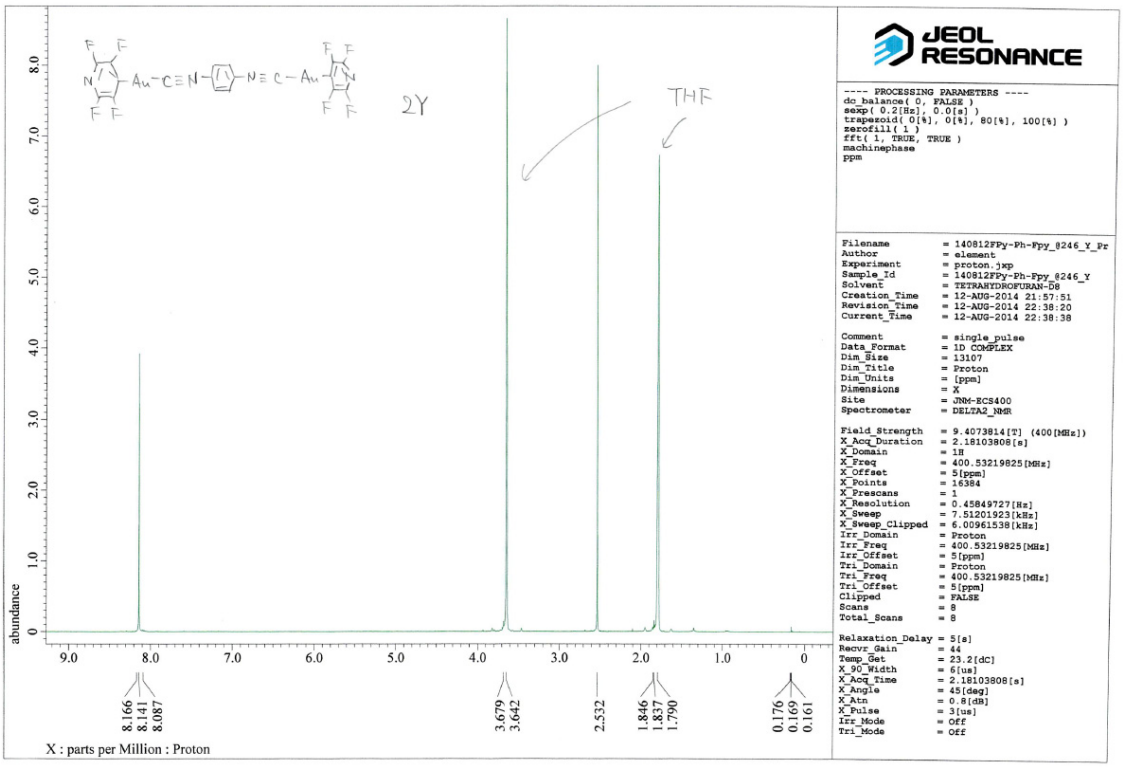

Fig. S13 ^{1}H NMR spectrum of **2Y** dissolved in THF-d_8.

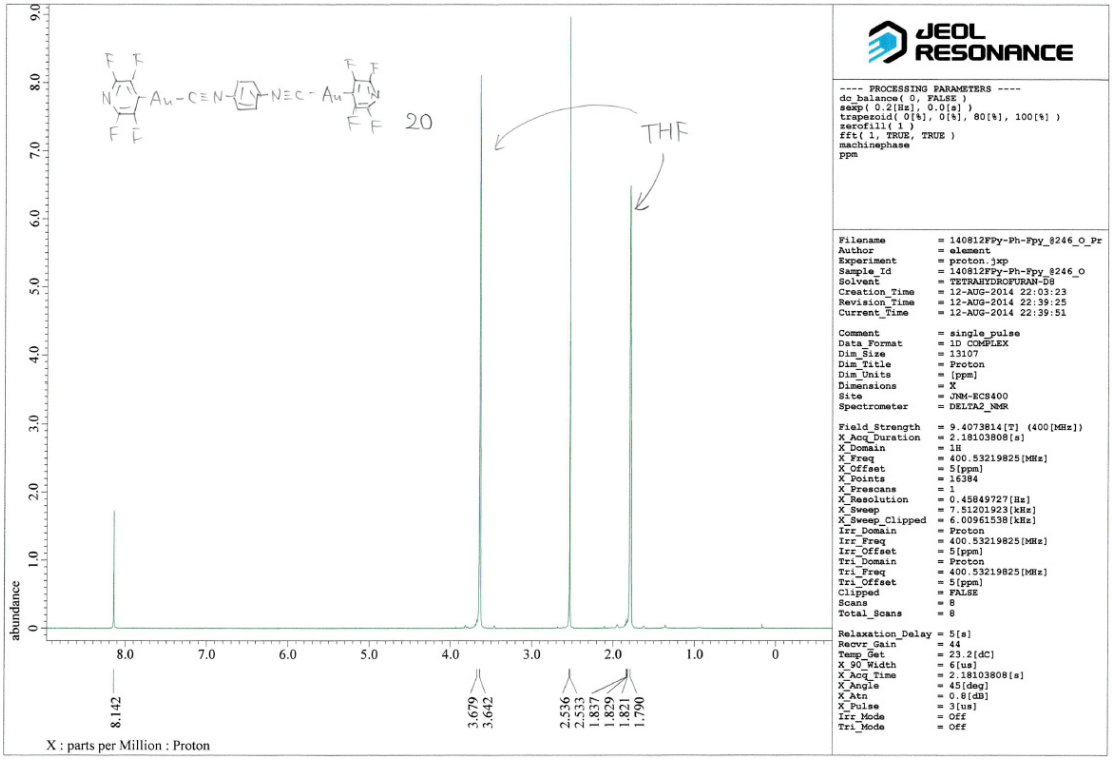

Fig. S14 ^{1}H NMR spectrum of **2O** dissolved in THF-d_8.

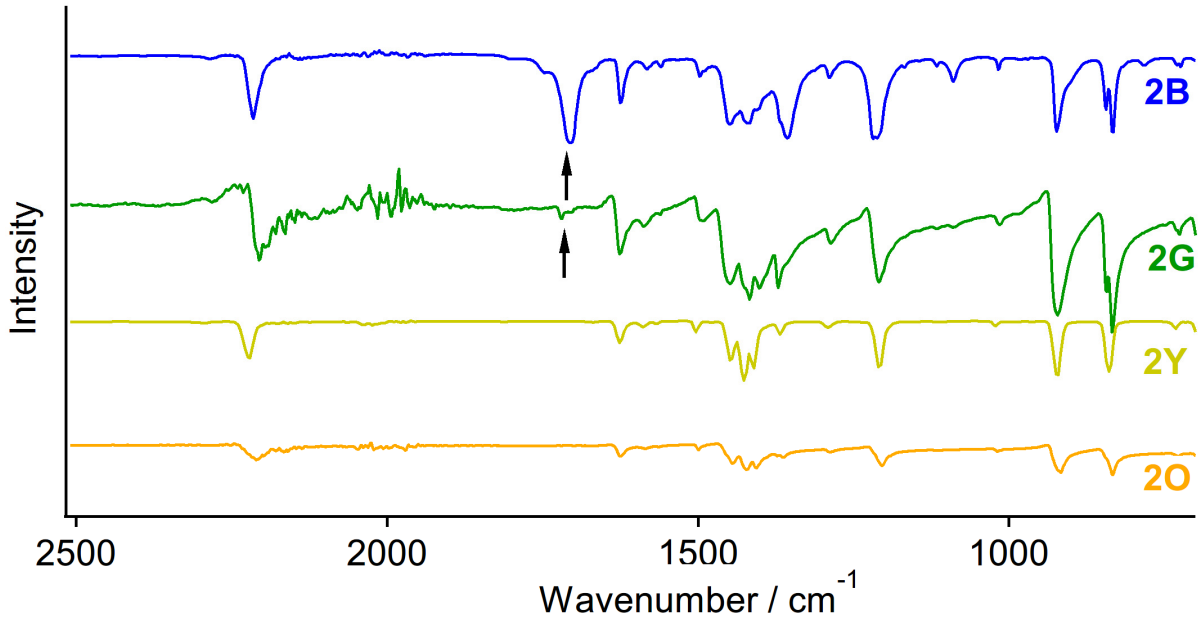

Fig. S15 IR spectra of **2B**, **2G**, **2Y**, and **2O.** Arrows indicate C=O stretching vibration bands of acetone that was included in the crystalline lattice.

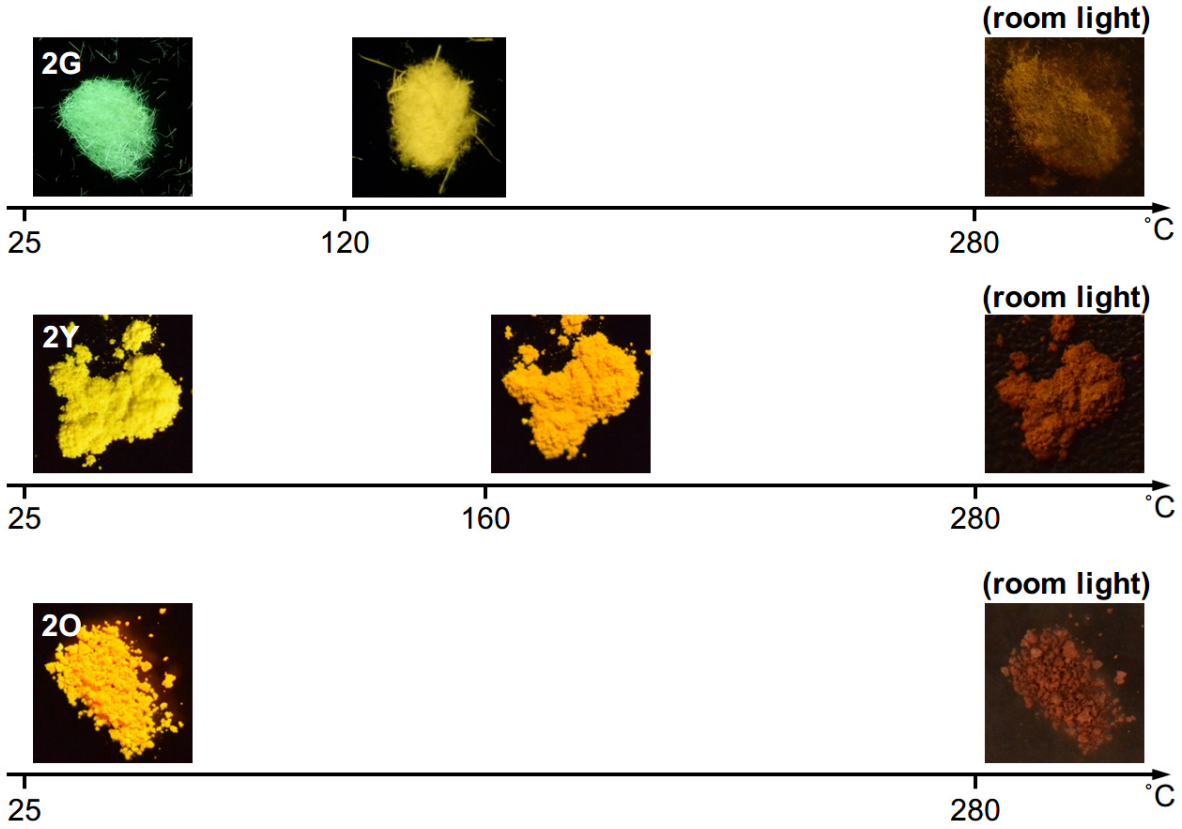

Fig. S16 Photographs of **2G**, **2Y**, and **2O** under UV light otherwise denoted and their thermal induced emission color changes.

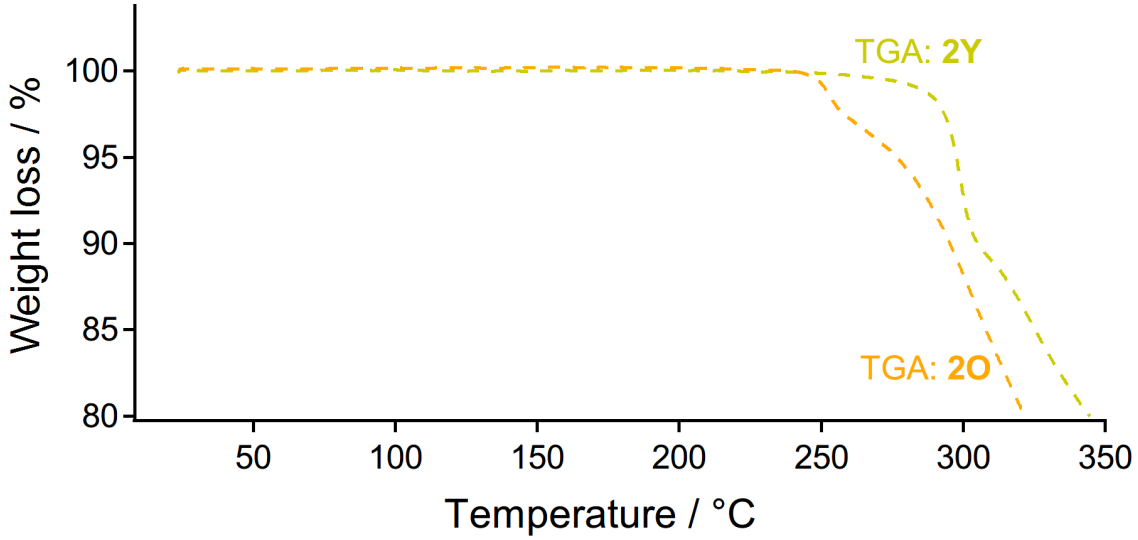

Fig. S17 TGA profiles of **2Y** (dashed yellow lines) and **2O** (dashed orange lines) at a heating rate of 10 °C/min.

Table S4 Elemental analyses of **2B**, **2G**, **2Y**, and **2O**.

	C	H	N
Calculated for **2** ($C_{18}H_4Au_2F_8N_4$)	26.30	0.49	6.81
2B (solvated polymorph)	–	–	–
2G (solvated polymorph)	26.67	0.89	6.66
2Y (solvent-free polymorph)	26.39	0.60	6.79
2O (solvent-free amorphous phase)	26.23	0.64	6.63

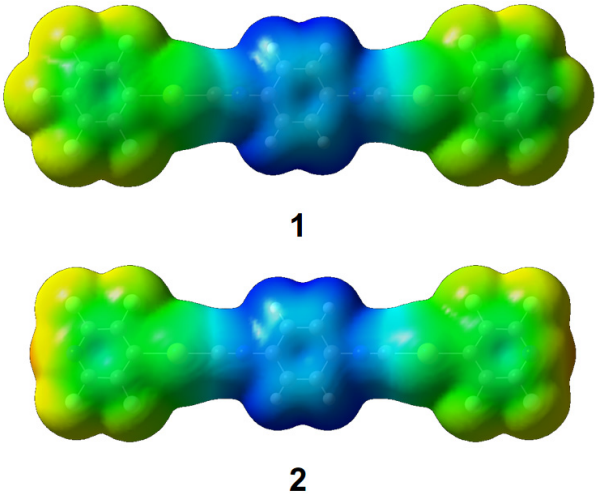

Fig. S18 Surface charge distribution of **1** and **2** calculated by means of DFT method (B3LYP/SDD).

7. References

S1. http://www.ccdc.cam.ac.uk/free_services/mercury/downloads/Mercury_3.0/

S2. Sheldrick, G. M. Acta Crystallogr., Sect. A 2008, 64, 112.

S3. Spek, A. L. PLATON99, A Multipurpose Crystallographic Tool, 1999.

S4. A. Boultif and D. Lou€er, J. Appl. Crystallogr., 2004, 37, 724–731.

S5. P. M. Wolff, J. Appl. Crystallogr., 1972, 5, 243.

S6. G. S. Smith and R. L. Snyder, J. Appl. Crystallogr., 1979, 12, 60–65.

S7. G. S. Pawley, J. Appl. Crystallogr., 1981, 14, 357–361.

S8. W. I. F. David, K. Shankland, J. Van de Streek, E. Pidcock and S. Motherwell, DASH version 3.0, Cambridge Crystallographic Data Centre, Cambridge, U.K., 2004.

S9. H. M. Rietveld, J. Appl. Crystallogr., 1969, 2, 65–71.

S10. A. C. Larson and R. B. Von Dreele, GSAS, Los Alamos Laboratory, Report No. LA-UR-86-748, Los Alamos National Laboratory, Los Alamos, NM, 1987.